Solid State Science and Technology, Vol. 13, No 1 & 2 (2005) 304-321
ISSN 0128-7389

MAGNETIC, MICROSTRUCTURE AND ELECTRICAL BEHAVIOUR OF SOME $(Li_{0.5}Fe_{0.5})_{0.7-x}Ni_xZn_{0.3}Fe_2O_4$ FERRITES

A. N. Yusoff and M. H. Abdullah

Diagnostic Imaging and Radiotherapy Programme,
Faculty of Allied Health Sciences,
Universiti Kebangsaan Malaysia,
50300 Jalan Raja Muda Abdul Aziz, Kuala Lumpur.
*Physics Programme, School of Applied Physics,
Faculty of Science and Technology,
Universiti Kebangsaan Malaysia,
43600 Bangi, Selangor Darul Ehsan.

ABSTRACT

The effects of substituting $(Li^{+}_{0.5}Fe^{3+}_{0.5})$ ions with Ni^{2+} ion on microstructural, magnetic, d.c. and a.c. electrical properties of some polycrystalline $(Li_{0.5}Fe_{0.5})_{0.7-x}Ni_xZn_{0.3}Fe_2O_4$ ferrites were studied. The d.c. electrical resistivity (ρ_{dc}) at 300 K increases with Ni content, while the experimental density (d), saturation magnetisation (M_s), initial permeability (μ_i) and Neel Temperature (T_N) show otherwise. The variations of magnetic and electrical properties are explained on the basis of cation distribution between the tetrahedral (A) and octahedral (B) sites. The complex impedance measurement was performed at different input voltage in ten decades of frequency (1 mHz - 10 MHz). The impedance spectrum for all samples is composed of two overlapping semicircles with negative capacitance phenomenon below approximately 1 Hz. However, the negative capacitance phenomenon is absent for x = 0.7. The two semicircles at high and low frequencies are mainly attributed to the grain (b) and grain boundary interfacial (g) processes respectively. The grain boundary interfacial response shows a non-linear dependence on the input voltage, where the corresponding impedance semicircle is smaller for a larger amplitude. However, a linear response is observed for the grain component. Simulation on the impedance data was performed using a complex nonlinear least square (CNLS) fitting method based on an equivalent circuit representation. The simulated quantities are the physical parameters of the microstructural components for the ferrites. The dependences of the a.c. electrical properties of the grain and the grain boundary interfacial components on composition and the amplitude of the input voltage are discussed.

INTRODUCTION

Spinel ferrites are soft magnetic oxides containing iron ions as a major constituent. They crystalised in a cubic spinel structure in which a face-centered close-packed lattice of oxygen ions contains one or more divalent metal ions such as Mn^{2+}, Fe^{2+}, Ni^{2+}, Zn^{2+}, Mg^{2+}, Cd^{2+} or monovalent Li^{+} ions, being distributed over the tetrahedral (A) and

octahedral (B) interstitial sites. The structure is normal spinel if all of the metal ions are in the A sites and the trivalent iron ions are in the B sites. However, many of the ferrites are inverse spinel where the divalent metal ions are in the B sites and the trivalent iron ions are equally distributed between the A and B sites. Most of the commercially fabricated ferrites are mixed ferrites containing two or three different kind of divalent metal ions, for example Mn-Zn, Mn-Mg-Zn, Ni-Zn, Li-Ni and Ni-Cd-Zn ferrites. Mixed ferrites with small power loss and high dielectric constant, resistivity and initial permeability can be prepared through a systematic substitution of several cations in the composition. Intensified research on the properties of ferrite materials substituted with various cations have been carried out by many workers [1-3]. These materials find various applications over a wide range of frequency from mHz to GHz range. In the field of microwave, works are focussed on developing new microwave-absorbing materials with higher efficiency [4-6].

In this work, microstructural, magnetic, d.c. and a.c. electrical properties of some polycrystalline $(Li_{0.5}Fe_{0.5})_{0.7-x}Ni_xZn_{0.3}Fe_2O_4$ ferrites were studied. Structural and microstructural studies were carried out using an X-ray diffractometer and an electron microscope. Magnetic quantities such as saturation magnetisation (M_s), remanent magnetisation (M_r), coercivity (H_c) and initial permeability (μ_i) were evaluated from the initial magnetisation and the hysteresis curves. The Neel temperature was determined from the magnetisation versus temperature curve. In the CIS technique, the effects of varying the amplitude of the input voltage on the grain and grain boundary interfacial responses are discussed in detail and the corresponding mechanisms of polarisation in the ferrites at high and low frequencies are determined. The complex impedance spectroscopy and a direct microstructural study using SEM are complementary, thus a complete characterisation and understanding of the microstructural properties of the materials can be made.

EXPERIMENTAL DETAILS

Samples of polycrystalline $(Li_{0.5}Fe_{0.5})_{0.7-x}Ni_xZn_{0.3}Fe_2O_4$ ferrites (x = 0, 0.1, 0.2, 0.3, 0.4, 0.5, 0.6 and 0.7) were prepared by a conventional sintering method from NiO, ZnO Li_2O and Fe_2O_3 powders of high purity (5N). The oxides were weighed, mixed and ground thoroughly in the desired stoichiometric composition together with 0.5 wt % of Bi_2O_3. The mixture was calcined at 800 °C for 6 hours and subsequently furnace-cooled to room temperature. The partially reacted mixture was then reground and pelletised into a disc-shaped form of 13 mm in diameter and 2 mm in thickness at a pressure of about 50 MPa. A small quantity of polyvinyl alcohol (PVA) was added as a binding agent. The pellet was subsequently sintered at 1050 °C for 15 hours and then slowly cooled in a similar manner. The addition of Bi_2O_3 and the use of lower calcining and sintering temperatures have been previously suggested [7, 8] for lithium and lithium-based ferrites in order to avoid vapourisation of the lithium and zinc as well as to increase the density and improve homogeneity of the ferrites. The experimental density was measured using Archimedes principle. The sample was immersed in glycerol ($CH_2OH.CHOH.CH_2OH$) and the density (d) was calculated from the relation $d = (W_a/W_g)d_g$, with W_a = weight of the sample in air, W_g = weight of the sample in glycerol and d_g = density of glycerol (1.255 g/cm^3). X-ray diffraction

(XRD) on the ferrite powder was carried out using a Siemens D5000 Diffractometer with CuKα_1 radiation (λ = 1.541 Å). The X-ray density (d_{XRD}) was calculated from the relation $d_{XRD} = 8M/N_o a^3$, where M = relative mass number, N_o = Avogadro's constant and a = lattice parameter. The morphological study was performed by a Philips XL 30 scanning electron microscope (SEM) at 1200x magnification. Sample for SEM was ground and polished using a Buehler grinder-polisher machine and etched at 1060º C for about two hours.

The magnetisation versus magnetic field (H_{max} = 5 kOe) and magnetic hysteresis at room temperature (R_T = 300 K) were measured by means of a vibrating sample magnetometer (VSM Model LDJ 9600). The saturation magnetisation for each sample was derived from the initial magnetisation curve while T_N is determined from the magnetisation versus temperature curve in a constant magnetic field of 100 Oe. The d.c. electrical resistivity measurement was made by a two-terminal method using a spring-loaded stainless steel electrodes (Ando Type SE-70) connected to an electrometer (Model Keithley 619). Silver paste was deposited onto both surfaces of the pellet to reduce contact resistance between the sample and the electrodes.

A frequency response analyzer (Solartron HF 1255) was used in the measurement of the real (Z') and imaginary (Z'') parts of the complex impedance ($Z^* = Z' - jZ''$) for the samples. The measurement was performed at room temperature over a frequency range of 1 mHz to 10 MHz. In this technique the sample is subjected to a sinusoidal voltage and the resulting current together with the phase difference between the input voltage and the current were measured and analysed. The a.c. signals with amplitudes of 0.5 V, 1.0 V, 1.5 V and 2.0 V were produced by a locked-in signal generator in the HF 1255. The impedance measurement was performed at different input voltage amplitudes in order to investigate the presence of non-linearity in the a.c. electrical response of the material. It has been proposed [9] that linearity condition is fulfilled if the measured impedance spectrum does not depend on the amplitude of the input voltage. The impedance data were analysed using a complex nonlinear least square fitting method (CNLS). The good fitting criteria were associated with the smallest values of the target function (χ^2) and the standard deviation (S), where $\chi^2 = \Sigma[(Z_{e,i} - Z_{s,i})^2/Z_i]$ with $\chi'^2 = \Sigma[(Z'_{e,i} - Z'_{s,i})^2/Z'_{s,i}]$, $\chi''^2 = \Sigma[(Z''_{e,i} - Z''_{s,i})^2/Z''_{s,i}]$, $S' = \sqrt{(1/N)\Sigma}(Z'_{e,i} - Z'_{s,i})^2$ and $S'' = \sqrt{(1/N)\Sigma}(Z''_{e,i} - Z''_{s,i})^2$. $Z'_{e,i}$ and $Z''_{e,i}$ are the real and imaginary impedances for the i^{th} experimental data at a frequency of ω_i, while $Z'_{s,i}$ and $Z''_{s,i}$ are the simulated values of these quantities. The subscript i is taken from 1 to N, where N is the number of data to be analysed. Since the geometrical factor of the ferrite samples are not the same, in certain cases it is more convenience to present the impedance results in the form of complex resistivity so that a meaningful comparison regarding the materials properties can be made. The corresponding complex resistivity of the sample is $\rho^* = \rho' - j\rho''$ where $\rho' = Z'A/t$ and $\rho'' = Z''A/t$, where A and t are the cross-sectional area and thickness of the sample respectively.

Solid State Science and Technology, Vol. 13, No 1 & 2 (2005) 304-321
ISSN 0128-7389

RESULTS AND DISCUSSION

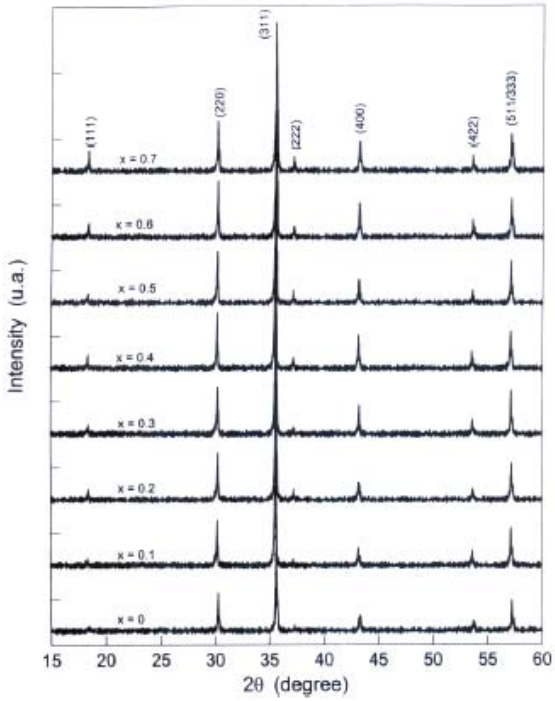

Figure 1: X-ray diffraction patterns for $(Li_{0.5}Fe_{0.5})_{0.7-x}Ni_xZn_{0.3}Fe_2O_4$ ferrite samples (x = 0, 0.1, 0.2, 0.3, 0.4, 0.5, 0.6 and 0.7) showing the presence of the characteristic planes of a cubic spinel structure.

The X-ray diffraction patterns obtained at room temperature for the $(Li_{0.5}Fe_{0.5})_{0.7-x}Ni_xZn_{0.3}Fe_2O_4$ ferrite system (x = 0, 0.1, 0.2, 0.3, 0.4, 0.5, 0.6 and 0.7) are depicted in Fig. 1. The patterns confirm the presence of all characteristic planes of the cubic spinel structure. Each diffraction peak was indexed using the relation $\sin^2\theta/(h^2 + k^2 + l^2) = \lambda^2/4a^2$, where θ = Bragg angle, (h k l) = Miller indices, λ = wavelength of the X-ray (1.541 Å) and a = lattice parameter. The equation is a combination of the Bragg's law and the plane spacing equation. For a cubic crystal, each diffraction line can only has one set of (h k l) corresponding to one $\sin^2\theta$ value. The main reflection planes are (111), (220), (311), (222), (400), (422), (511/333) and (440). The lattice parameter (a) calculated from the XRD data, as shown in Table 1, increases slightly with increasing Ni content. This is attributed to the replacement of smaller xLi^+ ions (0.60Å) and xFe^{3+} ions (0.64Å) by $2xNi^{2+}$ ions of larger ionic radius (0.72Å). The results compared favourably with those obtained by Kishan et al. [7] and Mitra et al. [8]. The bulk experimental density (d) for the samples was found to be in between 4.50 - 5.00 g/cm^3. The SEM micrographs for some $(Li_{0.5}Fe_{0.5})_{0.7-x}Ni_xZn_{0.3}Fe_2O_4$ ferrites (x = 0, 0.1, 0.2, 0.4 and 0.5) at 1200x magnification are shown in Fig. 2. It can be seen that the samples are characterised by grains which are separated by grain boundaries and voids. It seems that the size of the grains are not uniform for all samples. The X-ray density increases with Ni content because the increase in the mass of a unit cell predominates over the increase in its volume. The porosity of the samples calculated

from the X-ray and the bulk experimental densities was found to be increasing with Ni content. This seems to be consistent with the micrographs shown in Fig. 2.

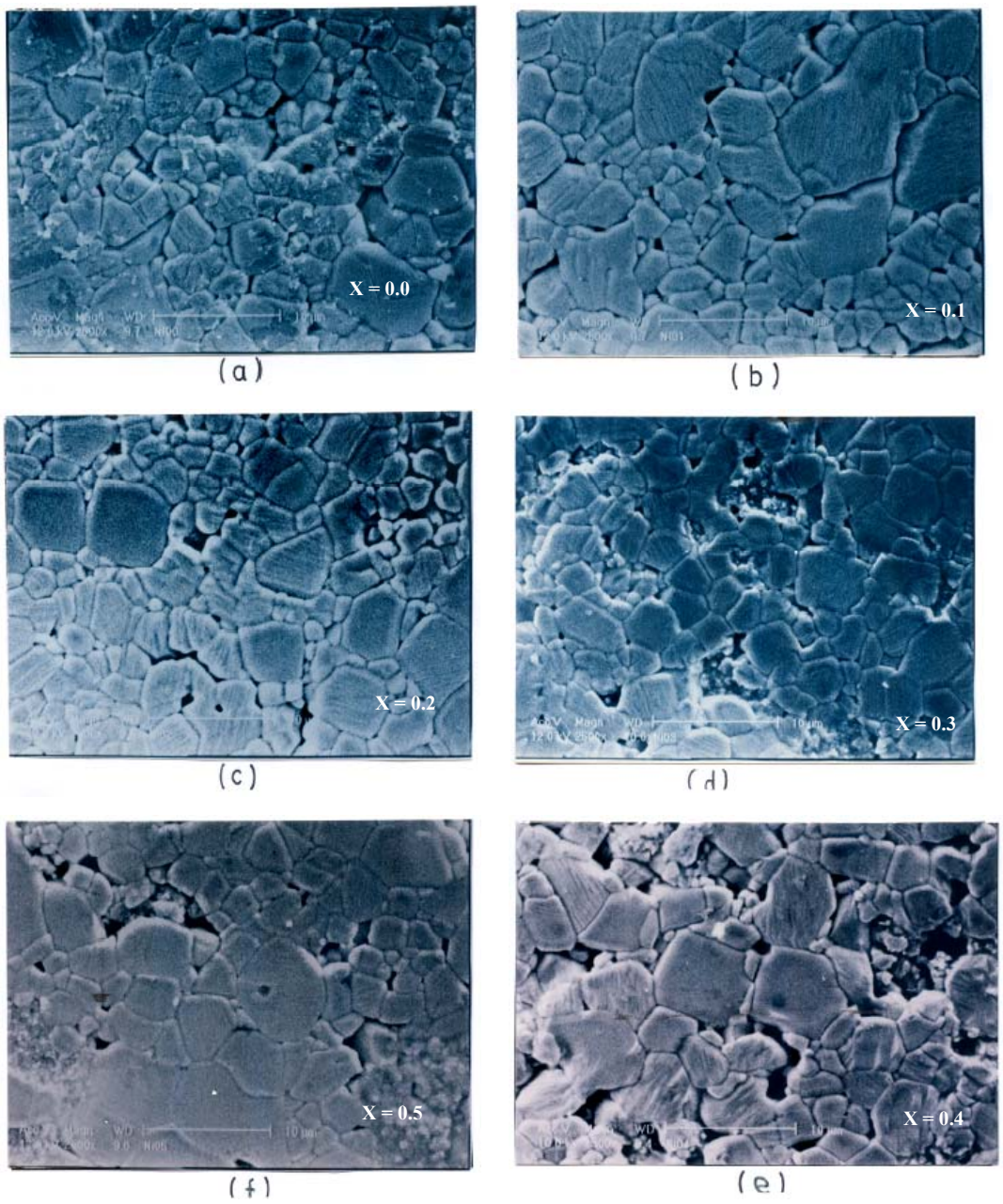

Figure 2 SEM micrographs for $(Li_{0.5}Fe_{0.5})_{0.7-x}Ni_xZn_{0.3}Fe_2O_4$ ferrite samples; (a) x = 0, (b) x = 0.1, (c) x = 0.2, (d) x = 0.4 and (e) x = 0.5.

Solid State Science and Technology, Vol. 13, No 1 & 2 (2005) 304-321
ISSN 0128-7389

Table 1 : Some characteristic parameters obtained from structural, d.c. electrical and magnetic measurements on $(Li_{0.5}Fe_{0.5})_{0.7-x}Ni_xZn_{0.3}Fe_2O_4$ ferrites (x = 0, 0.1, 0.2, 0.3, 0.4, 0.5, 0.6 and 0.7) at room temperature. The ferrites were fired at 1050 °C for 15 hours.

x	0	0.1	0.2	0.3	0.4	0.5	0.6	0.7
Rel. mass number	217	220	223	226	228	231	234	236
a (± 0.001 Å)	8.347	8.351	8.354	8.356	8.359	8.364	8.371	8.377
d (± 0.01 g/cm^3)	4.92	4.88	4.83	4.76	4.69	4.64	4.59	4.53
d_{XRD} (± 0.01 g/cm^3)	4.97	5.02	5.08	5.14	5.19	5.25	5.30	5.34
Porosity (± 0.5 %)	1.0	3.0	5.0	7.0	10.0	12.0	13.0	15.0
ρ_{dc}(± 0.01 x 10^5 Ω.cm)	0.98	1.20	8.21	13.07	18.91	26.57	52.38	448.54
M_s (± 0.1 emu/g)	86.2	83.9	82.5	82.1	79.9	78.9	77.7	73.4
μ_i (± 5)	555	305	115	55	50	45	35	20
M_r (± 0.01 emu/g)	0.13	0.19	0.26	0.32	0.36	0.38	0.40	0.41
H_c (± 0.01 Oe)	0.32	0.35	0.53	1.01	1.41	1.58	1.66	1.73
T_N (± 5 °C)	750	740	720	715	710	705	695	675

The basic composition of the ferrites under study is $Li_{0.5}Fe_{2.5}O_4$. Braun [10] was the first to show that the ferrite with this composition is an inverse spinel where the cation distribution can be represented as $[Fe^{3+}]^A[Li^+_{0.5}\ Fe^{3+}_{1.5}]^B$ where the superscripts A and B denote the tetrahedral and octahedral sites respectively. The divalent ion in this case being a composite ion of $(Li^+_{0.5}Fe^{3+}_{0.5})$. Since lithium ion is monovalent, it enters the lattice in combination with an Fe^{3+} ion in order to balance the charge and minimise the total electrostatic energy in the lattice. When $z(Li^+_{0.5}Fe^{3+}_{0.5})$ composite ions are substituted with zZn^{2+} ions, a new cation distribution is formed. The zZn^{2+} ions predominantly enter the A sites, hence transfering zFe^{3+} ions to the B sites. Thus, the new cation distribution can be written as $[Zn^{2+}_zFe^{3+}_{1-z}]^A[(Li^+_{0.5}Fe^{3+}_{0.5})_{1-z}Fe^{3+}_{1+z}]^B$ [7]. The Zn^{2+} subtitution has beneficial influences on the magnetic properties, the microstructure and densification of the bulk materials. Table 2 shows some magnetic and d.c. electrical resistivity data of some $(Li^+_{0.5}Fe^{3+}_{0.5})_{1-z}Zn_zFe_2O_4$ ferrites measured at room temperature. These ferrites were prepared without Bi_2O_3 addition and were sintered at 1230°C for 20 hours. The initial increase in the magnetisation as a function of Zn content is expected from the increase in magnetic interaction between the A and

B sites. The magnetisation reaches a maximum value at z = 0.3 and thereafter decreases as zinc ferrite is approached. The d.c. electrical resistivity for these ferrites is quite low where the value was found to be in the order of 10^4 Ω.cm. This is mainly attributed to the higher content of Fe^{2+} ion. The ferrites were sintered at 1230°C for 20 hours and this would vapourise a large amount of Li^+ and Zn^{2+} ions which results in the reduction of Fe^{3+} ions to Fe^{2+} ions.

Table 2 : Some magnetic and d.c.electrical properties of $(Li_{0.5}Fe_{0.5})_{1-z}Zn_zFe_2O_4$ ferrites (z = 0.2, 0.3 and 0.4) at room temperature. The ferrites were prepared without any Bi_2O_3 addition and were sintered at 1230° C for 20 hours.

z	M_s (± 0.1 emu/g)	M_r (± 0.01 emu/g)	H_c (± 0.01 Oe)	ρ_{dc} (± 0.1 x 10^4 Ω.cm)
0.2	83.2	0.39	1.32	1.5
0.3	86.2	0.12	2.10	2.4
0.4	81.4	0.13	0.06	2.0

When x fraction of the composite $(Li^+_{0.5}Fe^{3+}_{0.5})$ from the sample with the highest magnetisation in Table 2 (z = 0.3) is substituted with xNi^{2+}, the resulting cation distribution can be written as $[Zn^{2+}_{0.3}Fe^{3+}_{0.7}]^A[(Li^+_{0.5}\ Fe^{3+}_{0.5})_{0.7-x}Ni^{2+}_xFe^{3+}_{1.3}]^B$. This is true since Ni^{2+} ion has a tendency to enter the octahedral site by replacing the composite $(Li^+_{0.5}Fe^{3+}_{0.5})$. The effect of Bi_2O_3 addition and the use of a lower sintering temperature can be seen by comparing the sample x = 0 in Table 1 and the sample z = 0.3 in Table 2. Their compositions are identical but nevertheless their magnetic and electrical properties are different. The sample x = 0 in Table 1 posseses higher electrical resistivity with lower M_s and H_c. However, the M_r values for both samples are about the same. The d.c. electrical resistivity (ρ_{dc}) for the ferrites in Table 1 was also found to be increasing with Ni content. A higher resistivity is due to a lower Fe^{2+} content in the materials. The concentration of Fe^{2+} ions is assumed to be proportional to the concentration of Fe^{3+} ions. As mentioned before, most of the Fe^{2+} ions result from the reduction of Fe^{3+} ions during sintering process. It seems that the preparation of the ferrites at a lower sintering temperature with the addition of Bi_2O_3 had prevented excessive formation of Fe^{2+} ion. The variations of the d.c. resistivity, saturation magnetisation, initial permeability, remanent magnetisation and coercivity as a function of Ni content (x) are shown in Table 1. It is observed that M_s decreases, but M_r and H_c tend to increase, with increasing Ni content. The decrease in M_s for higher Ni content is attributed to the decrease in the net magnetic moment in the B sublattice. The Ni^{2+} ion possess a magnetic moment of 2 μ_B whereas Fe^{3+} ion possess a higher magnetic moment of 5 μ_B, hence the substitution of $x(Li^+_{0.5}Fe^{3+}_{0.5})$ ions with xNi^{2+} in the B sites

results in an overall decrease in magnetisation. The values of M_r and H_c indicate that the ferrites are soft magnetically. A very narrow hysteresis loop for all samples at room temperature indicates that magnetic energy loss in the process is very small. Samples with higher saturation magnetisation possess lower values of M_r and H_c. Table 2 also indicates that the substitution of $(Li^{+}_{0.5}Fe^{3+}_{0.5})$ ions with Ni^{2+} ions lowers μ_i. The initial permeability is calculated from the initial slope of the magnetisation curve, which is the change of the magnetic induction (B) with respect to the magnetic field intensity (H) as H approaches zero. Samples with higher initial permeability are those that posses higher saturation magnetisation, higher Li^{+} and Fe^{3+} content and lower porosity. These factors enhance domain wall motion and the alignment of the magnetic moments when the field is applied. According to Went and Wijn [11] the initial permeability of ferrites is related to the saturation magnetisation and the anisotropy constant (K) in such a way that $(\mu_i - 1)/4\pi = 2M_s^2/3K$. It seems that the increase in M_s predominates over the value of K for these ferrites.

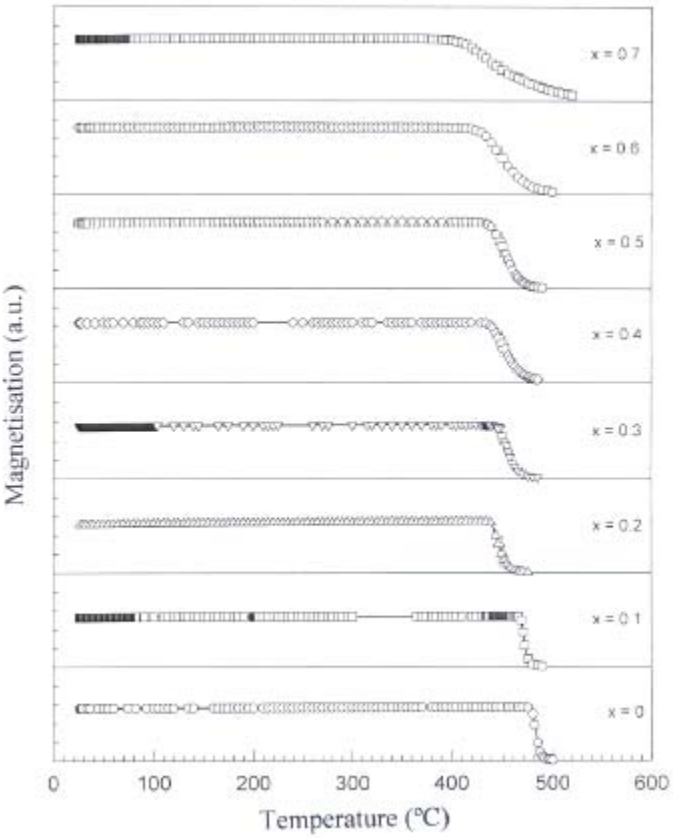

Figure 3: Magnetisation as a function of temperature for the ferrites. The measurement was performed under a constant magnetic field of 100 Oe.

Fig. 3 shows the plot of magnetisation as a function of temperature for all samples. The magnetisation was measured in a constant applied magnetic field (H_a) of 100 Oe. All samples exhibit a pronounce magnetic stability with increasing temperature up to 400 ° C. As the temperature is further increased, a sharp drop in magnetisation can be observed for all samples. The abrupt change in magnetisation which occurs at The Neel

temperature (T_N) corresponds to the change from ferrimagnetic to paramagnetic phases of the material. It can be seen that T_N increases with increasing Li content. A stronger exchange interaction resulting from a stronger magnetisation and a higher initial permeability for samples with higher Li content results in a stronger magnetic ordering in the materials. Therefore, a higher thermal energy is needed to overcome the exchange energy in the ferrimagnetic state, hence a higher T_N. The region just above T_N is known as critical region which is characterised by short range interactions between the magnetic ions. The increase in Fe^{2+} ions will increase the superexchange interaction between the Fe^{2+} and Fe^{3+} ions for electron conduction and magnetic interaction, so that the activation energy in the paramagnetic state is effectively reduced and the change from ferrimagnetic to paramagnetic state is sharp. If the concentration of Fe^{2+} ions is reduced to a certain level, the resistivity of the material and the paramagnetic activation energy are high resulting in a gradual decrease of magnetisation on passing through T_N.
In general, polycrystalline ferrites are composed of good conducting grains separated by highly resistive grain boundaries. This model has been used by several workers [3, 7] to describe dielectric relaxation in some lithium-based ferrites. The model assumed that at any frequency, both the grains and grain boundaries simultaneously respond to the input sinusoidal voltage. However, at low frequencies, the impedance response from the grain boundaries and interfaces are large compared to the response from the grain so that the space charge polarisation is dominant. At frequencies above 100 kHz, the space charge polarisation is out of phase with the applied field resulting in a relaxation. The space charge response is then overtaken by the grain response which is dominated by orientational polarisation at very high frequencies.

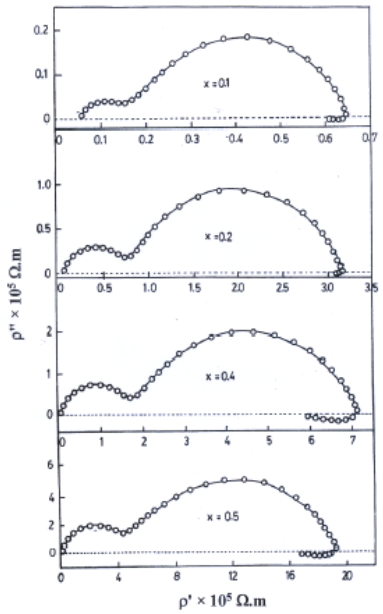

Figure 4(a): The complex-plane resistivity spectrum for $(Li_{0.5}Fe_{0.5})_{0.7-x}Ni_xZn_{0.3}Fe_2O_4$ ferrites (x = 0.1, 0.2, 0.4 and 0.5) in the frequency range of 1 mHz - 10 MHz at the input voltage of 2V. All measurements were performed at room temperature.

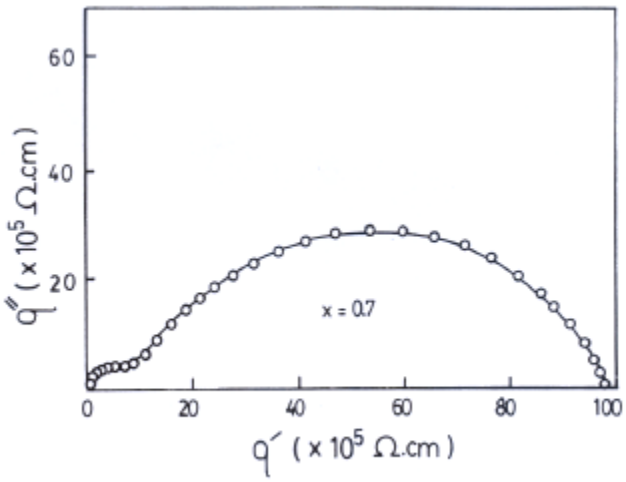

Figure 4(b): The complex-plane resistivity spectrum for $(Li_{0.5}Fe_{0.5})_{0.7-x}Ni_xZn_{0.3}Fe_2O_4$ (x = 0.7). in the frequency range of 1 mHz - 10 MHz at the input voltage of 2V.

Fig. 4(a) offers a series of complex resistivity plots of $(Li_{0.5}Fe_{0.5})_{0.7-x}Ni_xZn_{0.3}Fe_2O_4$ ferrites (x = 0.1, 0.2, 0.4 and 0.5) at 2V input voltage amplitude. The spectrum are characterised by two partially overlapping semicircles at high and low frequencies due to two different conduction-polarisation processes in the material as mentioned above. This type of response in the same frequency range has been observed for some ferrite materials [13, 14]. The spectrum for $Li_{0.35}Zn_{0.3}Fe_{2.35}O_4$ ferrite (shown in Fig. 7) is seen to compose of only one semicircle. However, it is believed that the two semicircles largely overlapped each other. According to Kleitz and Kennedy [23] on the analysis of the multicomponent impedance distribution, a considerable overlapping of two impedance semicircles on a complex-plane is observed if the ratio of the time constants of the low-frequency to the high frequency semicircles is less than two orders of magnitude.

Solid State Science and Technology, Vol. 13, No 1 & 2 (2005) 304-321
ISSN 0128-7389

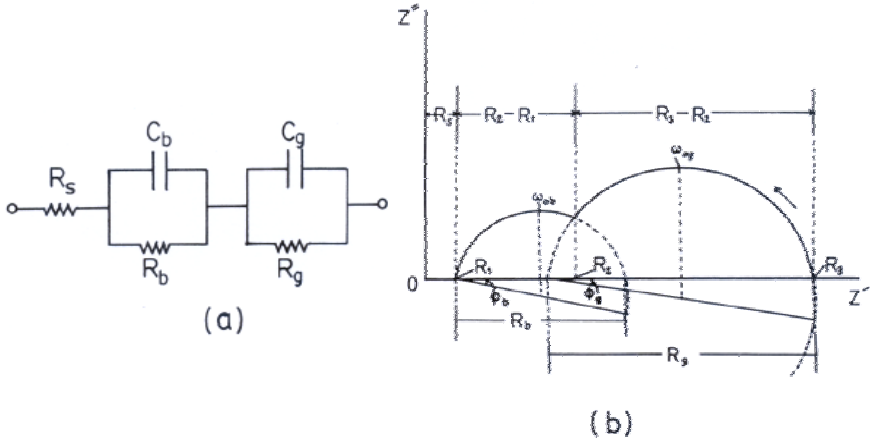

Figure 5: a) The proposed equivalent circuit model for the ferrites and b) the sketch of a complex impedance spectrum showing various parameters discussed in the text.

In the present study, an equivalent circuit representation is used as an essential step towards a better understanding of the material properties. We proposed as in our previous works on some Mg-Zn ferrites [13,14], an equivalent circuit which produces the same impedance response. The circuit consists of a resistor (R_s) in series with two parallel R-C loops, see Fig. 5(a). The inclusion of R_s is to account for the shift in the origin of the impedance spectrum. It has been proven that the use of different materials for electrodes or holders, such as cooper or stainless steel, was found to have a small effect on R_s or the shift of the spectrum along Z' axis. The two R-C loops correspond to two major types of electrical response from the grain and grain boundary interfacial components. C_b and C_g in the circuit are the grain and the grain boundary interfacial frequency-dependent "non-Debye" capacitive elements, while R_b and R_g are their respective resistances. The inclusion of the capacitive and resistive elements in the circuit is to represent the polarisation and the conduction processes in the materials when subjected to a sinusoidal potential. Further analysis on the impedance spectrum will be focussed on two semicircles denoted by "b" for the grain and "g" for the grain boundary interfacial components with the understanding that the grain boundary and ferrite-electrodes responses at low frequencies are not individually separated on the complex plane. Thus the corresponding impedance expression for the case of two overlapping semicircles is given by

$$Z^*(\omega) = R_s + \frac{R_b}{1 + (i\omega\tau_{ob})^{1-\alpha_b}} + \frac{R_g}{1 + (i\omega\tau_{og})^{1-\alpha_g}} \quad (1)$$

where

Solid State Science and Technology, Vol. 13, No 1 & 2 (2005) 304-321
ISSN 0128-7389

$$Z'(\omega) = R_s + \frac{R_b[1 + (\omega\tau_{ob})^{1-\alpha_b} \sin(\alpha_b\pi/2)]}{1+2(\omega\tau_{ob})^{1-\alpha_b} \sin(\alpha_b\pi/2) + (\omega\tau_{ob})^{2(1-\alpha_b)}} + \frac{R_g[1 + (\omega\tau_{og})^{1-\alpha_g} \sin(\alpha_g\pi/2)]}{1+2(\omega\tau_{og})^{1-\alpha_g} \sin(\alpha_g\pi/2) + (\omega\tau_{og})^{2(1-\alpha_g)}} \quad (2)$$

and

$$Z''(\omega) = \frac{R_b(\omega\tau_{ob})^{1-\alpha_b} \cos(\alpha_b\pi/2)}{1+2(\omega\tau_{ob})^{1-\alpha_b} \sin(\alpha_b\pi/2) + (\omega\tau_{ob})^{2(1-\alpha_b)}} + \frac{R_g(\omega\tau_{og})^{1-\alpha_g} \cos(\alpha_g\pi/2)}{1+2(\omega\tau_{og})^{1-\alpha_g} \sin(\alpha_g\pi/2) + (\omega\tau_{og})^{2(1-\alpha_g)}} \quad (3)$$

In the above equations, α_b and α_g are the depression parameters which measure the deviation of the impedance plot from the ideal semicircular Debye-type of response for the grain and grain boundary interfacial regions respectively. The relation between the depression angles (ϕ_b and ϕ_g) and depression parameters (α_b and α_g) can be written as $\alpha_b = 2\phi_b/\pi$ and $\alpha_g = 2\phi_g/\pi$ ($\pi = 180°$). The values of α_b and α_g lie in between 0 and 1 as the possible values of ϕ_b and ϕ_g are in the range of 0° and 90°, where α_b and $\alpha_g = 0$ is the case of the ideal impedance distribution. R_b and R_g are the simulated values for the grain and grain boundary interfacial resistances. The mean relaxation times for the grain and grain boundary interfacial processes, $\tau_{ob} = R_bC_b$ and $\tau_{og} = R_gC_g$, are the inverse of the peak frequencies, ω_{ob} and ω_{og} respectively, so that C_b and C_g can be evaluated. Fig. 5(b) shows the sketch of the Z'' versus Z' with the corresponding parameters mentioned above. The results previously obtained from impedance measurements at several different temperatures for Mg-Zn [13] and Mn-Zn [15] ferrites supported the suitability and correctness of the equivalent circuit used. The measured and simulated grain and grain boundary interfacial resistances are found to decrease exponentially with temperature. This behaviour indicates that both the grain and grain boundary interfacial resistances are the characteristic properties of the ferrites that associated with a similar conduction mechanism. Apart from that, the simulated grain and grain boundary interfacial capacitances are almost constant with temperature. This is in the sense that under the influence of the external electric field, the same number of charge carriers is being transported through the grains and grain boundaries at all

temperatures. The experimental and simulated data for the sample x = 0.2 that satisfy the complex non-linear least square fitting (CNLS) criteria are shown in Fig. 6. The agreement between the measured and simulated impedance diagrams is good. A region of negative capacitance below 1 Hz, which will be discussed in the later section, is not represented in the equivalent circuit. The exclusion of the negative capacitance region only seems to exclude its existence in the simulated impedance curve, but the agreement between the measured and simulated impedances for the rest of the frequency range is maintained.

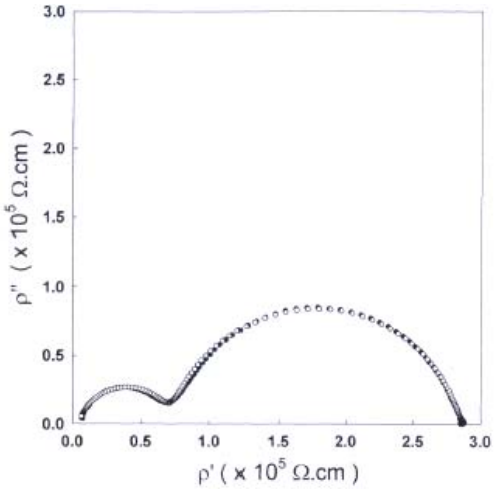

Figure 6: The experimental (filled symbols) and simulated (open symbols) spectra for x = 0.2 at two different input voltages.

The impedance spectrum of the present Li-Ni-Zn ferrites seems to be analogous to the behaviour of some polycrystalline ceramics [13 - 15]. Badwal [16] reported that the surface-electrodes interfacial process may occurs at frequencies lower than 1 kHz, while the grain boundary and the grain processes are usually observed in the frequency range of 1 kHz - 100 kHz and higher than 10 kHz respectively. The coupling of the impedance responses from the grain, the grain boundary and the surface-electrodes in these ferrites may occurs under certain microstructure. As for the Li-Zn ferrite, the compactness of the grains as suggested by the very low porosity and the higher content of Fe^{2+} ion are the reasons for the low resistivity of the material compared to the Li-Ni-Zn ferrites. The lower resistivity means a higher conductivity and polarisability in both the grain and grain boundary interfacial regions. These characteristics render the grain and the grain boundary interfacial responses indistinguishable on the complex plane. Hence, the two responses are completely overlapped or the impedance spectrum composed of only one semicircle. This is equivalent to the same relaxation time from the grain and grain boundary interfacial components. Thus, electrically, the Li-Zn ferrite resembles two R-C circuits as indicated in Fig. 5(a). It can be shown that the time constant of the complete circuit is given by $\tau = RC = (C_b + C_g)(R_bR_g)/(R_b + R_g)$ [17], where the combined capacitance C is given by $C = C_b + C_g \approx C_g$ since $C_b << C_g$. This is consistent with the measured possible capacitance for the sample, which is about 10^{-8} F (see Table 3). For other samples, it can be shown that the values of the grain and grain boundary interfacial capacitances for these ferrites are of the order of

10^{-11} F and 10^{-9} F respectively, which are the probable values for those processes in solid materials [18, 19].

Table 3 : Simulated parameters for $(Li_{0.5}Fe_{0.5})_{0.7-x}Ni_xZn_{0.3}Fe_2O_4$ ferrites obtained from the complex non-linear least square fitting (CNLS) method. The experimental data were taken at input signal of 2V at room temperature. The data for $x = 0$ were based on simulation on one impedance semicircle.

X	0	0.1	0.2	0.3	0.4	0.5	0.6	0.7
$R_s \pm 10\ \Omega$	1020	1030	1040	1050	1020	1040	1060	1030
ρ_b ($\pm$ 0.01 x $10^5\ \Omega$.cm)	-	0.09	0.54	1.01	1.68	5.20	9.60	14.10
ρ_g ($\pm$ 0.01 x $10^5\ \Omega$.cm)	0.02	0.47	2.20	4.81	5.10	13.60	52.00	89.50
ω_{ob} ($\pm$ 10 x 10^5 rad.s^{-1})	-	81.98	47.04	29.00	13.80	7.39	6.04	3.86
ω_{og} ($\pm$ 10 x 10^3 rad.s^{-1})	136.43	15.14	4.54	2.41	1.68	1.03	0.81	0.59
C_b ($\pm$ 0.01 pF)	-	76.04	21.27	20.24	19.27	15.02	12.12	9.075
C_g ($\pm$ 0.01 nF)	16.66	8.24	5.75	5.21	4.90	4.12	3.04	1.86
τ_{ob} ($\pm$ 0.01x 10^{-6} s)	-	0.12	0.21	0.35	0.73	1.35	1.66	2.59
τ_{og} ($\pm$ 0.01x 10^{-3} s)	0.01	0.07	0.22	0.42	0.60	0.97	1.24	1.70
ϕ_b ($\pm$ 1°)	-	15	13	11	10	12	13	15
ϕ_g ($\pm$ 1°)	5	15	13	12	15	14	15	23
α_b ($\pm$ 0.01)	-	0.17	0.14	0.12	0.11	0.13	0.14	0.17
α_g ($\pm$ 0.01)	0.06	0.17	0.14	0.13	0.17	0.16	0.17	0.26

The impedance plots for all samples indicate a region of negative capacitance below 1 Hz except for x = 0.7 (Fig. 4b). Jonscher [31] reported that the negative capacitance phenomenon at low frequencies is associated with a rising current in the step-function excitation in time domain response. It was discussed as due to the presence of a discontinuous interface between the sample and electrodes. Works by Baker and West [21] on the electrochemical impedance study of nickel-iron deposition reveal that the size of the inductive loop at low frequency of the impedance spectra change markedly with ferrous ion (Fe^{2+}) concentration. This is discussed as due to the adsorption of

intermediate ferrous ion species. The theory should be applicable to the ferrites since the sample with the lowest content of Fe^{3+} ion (x = 0.7) does not show any sign of negative capacitance or inductive loop at low frequency at all input voltages. It is assumed that the Fe^{2+} ion content in the ferrites is proportional to the starting composition of Fe^{3+} ion. However, further investigation on this subject is essential in order to ensure the validity of the present interpretation for the ferrites.

The d.c. electrical conduction in polycrystalline ceramics is due to percolation of charge carriers via a less resistive path. In ferrites the charge carriers are localised at the magnetic ions instead of occupying states in a wide energy band as in conventional semiconductors. The electrical conduction in ferrites normally results from the electron exchange between the trivalent and divalent iron ions, that is $Fe^{3+} + e \leftrightarrow Fe^{2+}$. The exchange of electron is dominant in octahedral sites since every octahedral Fe^{2+}/Fe^{3+} ion will has all its intersublattice magnetic bonds with other Fe^{2+}/Fe^{3+} ions; whereas each tetrahedral Fe^{2+}/Fe^{3+} ion will have on the average one half of its intersublattice magnetic bonds with other divalent metal ions and the other half with Fe^{2+}/Fe^{3+} ions. In the presence of an a.c. field, the electron exchange results in local displacement of the electrons in the direction of the alternating electric field. The electron conduction behave as the in-phase current flowing through the grains and grain boundaries. Table 3 shows a compositional dependence of various parameters obtained from the complex non-linear least square fitting method for the $(Li_{0.5}Fe_{0.5})_{0.7-x}Ni_xZn_{0.3}Fe_2O_4$ ferrites (x = 0, 0.1, 0.2, 0.3, 0.4, 0.5, 0.6 and 0.7) as described in the following sections. The system shows a considerable increase in both the grain and grain boundary interfacial resistivities (ρ_b and ρ_g) with increasing Ni content. The increase in ρ_{dc} (Table 1), ρ_b and ρ_g with Ni content is due to the reduction in the amount of Fe^{2+}/Fe^{3+} ion upon substituting $(Li^+_{0.5}Fe^{3+}_{0.5})$ ions with Ni^{2+} ions. A higher resistivity means a smaller capacitance since the polarizability of the materials is reduced with decreasing number of $(Li^+_{0.5}Fe^{3+}_{0.5})$ ions. It is also evident from Table 3 that the frequency at the peak of the respective semicircle (ω_{ob} and ω_{og}) is shifted to a lower value with increasing Ni content; hence resulting in a longer mean relaxation time (τ_{ob} and τ_{og}). The higher resistivity of the sample with higher Ni content would increase the duration of the relaxation process of the charge carrying species.

The relaxation process in the ferrites is deviated from the ideal Debye-type process since the centres of the impedance semicircles for the grain and grain boundary interfacial response are depressed to below the real axis. This shows that the polarisation and the conduction processes in the materials are strongly influenced by the environment of the charge carriers. This could be caused by the presence of interactions arising from the close proximity of atoms and molecules and by structural inhomogeneities such as lattice defects and impurities. The depression phenomenon in the Debye-like region has been elaborated by Jonscher based on the universal behaviour [22] where dielectric materials are presumed to show universality regardless of their physical and chemical properties and the nature of the polarising species. The theory was discussed in detail by Dissado and Hill [23,24]. The main result is that the dielectric loss is frequency-dependent such that $\varepsilon_r'' \propto \omega^{n-1}$, with $0 < n < 1$. A non zero value of n results in the suppression of the impedance semicircle and the broadening of Debye loss peak. The exponent n is almost temperature-independent. An interpretation

on the properties of some Mg-Zn ferrites [14] based on this concept has been found to be very useful. A similar discussion should be applicable for the present Li-Ni-Zn ferrite.

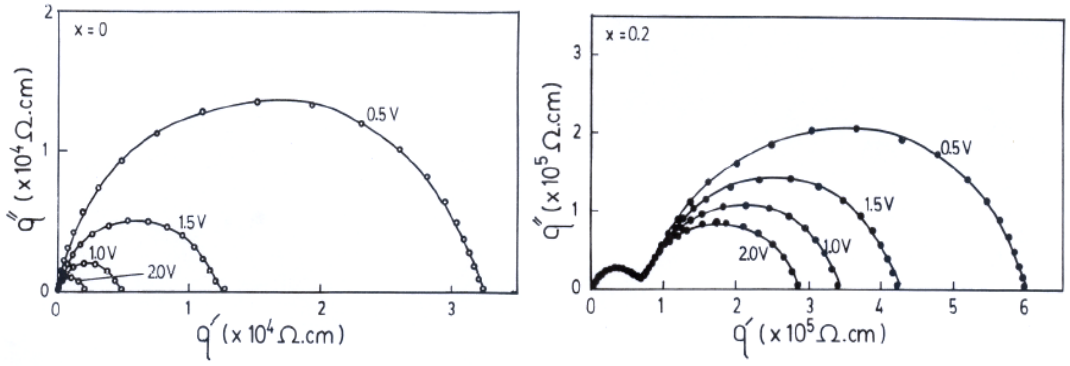

Figure 7: The complex-plane impedance spectra for $(Li_{0.5}Fe_{0.5})_{0.7-x}Ni_xZn_{0.3}Fe_2O_4$ ferrites (x = 0 and 0.2) measured at room temperature at different input signal amplitudes (0.5V, 1.0V, 1.5V and 2V) in the frequency range of 1 Hz - 10 MHz. The spectra indicate non-linearity of the grain boundary interfacial region with respect to the input signal amplitude.

Fig. 7 shows the complex-plane resistivity spectra for x = 0 and 0.2 at different amplitudes of the input voltage. It also shows a difference in the impedance response from the bulk and grain boundary interfacial regions. The grain component shows a linear behaviour as the size of the semicircle is independent of the input voltage. The a.c. electrical response of the grain region for the ferrite is said to be linear with respect to the amplitude of the input voltage if the ratio V(ω)/I(ω) which is equal to Z*(ω) remains constant throughout the frequency range of the grain response, where V(ω), I(ω) and Z*(ω) are the frequency dependence of the input voltage, current and complex impedance respectively. The linearity in the grain region is interpreted as due to the regularity in the structural properties and the uniformity in chemical composition of the grains. In contrast to this a strong departure from linearity is noticeable from the grain boundary interfacial response since the impedance semicircle is getting larger and the Z" peak is shifted towards lower frequency with the decrease in signal amplitude. The non-linear behaviour of the grain boundary interfacial response is discussed as due to the nature of the space charge polarisation in the regions. It has been discussed by Jonscher [31] that the strong influence of space charge on non-linearity lies in the fact that the injection and removal of the charge carriers are strongly non-linear, while the response of the dipoles such that in the grain remains essentially linear within a certain range of voltage. For the ferrites under study, the grain boundary interfacial resistance seems to decrease exponentially with the increase in input voltage. At higher input voltage a considerable amount of charge carriers is excited or released from the traps resulting in the increase in the a.c. conductivity. The non-linear increase in the quantity of the space charge carriers with the increase of the input voltage is a possible reason of the non-linear behaviour of the grain boundary interfacial component. Another interesting property is that the depression angles for both the grain and the grain boundary interfacial components seem to be independent to the amplitude of the input

voltage. It is thought that the environmental condition of the charge carriers is not influenced by the input voltage within the voltage range used in this work.

CONCLUSION

The $(Li_{0.5}Fe_{0.5})_{0.7-x}Ni_xZn_{0.3}Fe_2O_4$ ferrites investigated in this study are composed of well conducting grains surrounded by poorly conducting grain boundaries and voids. These ferrites posses high magnetisation with good temperature stability, high T_N and magnetic permeability with decreasing Ni content. However, a pronounce increase in the d.c. electrical resistivity with Ni is observed. The impedance response from the grain region is linear since it is independent of the amplitude of the input voltage. On the other hand the dependence of the impedance response of the grain boundary interfacial region on the amplitude of the signal shows that the a.c. electrical response of the region is non-linear. It is discussed that the non-linear increase in the quantity of the space charge carriers with the increase of the input voltage is a possible reason for the non-linear behaviour of the grain boundary interfacial component. The study assumes that the polarisation at lower frequencies (below 100 kHz) is dominated by the space charge polarisation in the grain boundary interfacial region, while at higher frequencies (above 100 kHz) the polarisation process is attributed to the Debye-like orientational polarisation. The a.c. complex impedance technique is useful for studying the electrical response and microstructural properties of the ferrite over a wide range of frequency. Simulation and the use of the complex non-linear least square fitting method is essential in analysing the properties of the material.

ACKNOWLEDGEMENT

This project is supported by a research grant IRPA 09-02-02-0005, of the Ministry of Science, Technology and Environment of Malaysia.

REFERENCES

[1] Prakash, C. (1987) *J. Mater. Sci. Lett.* **6**, 504.
[2] Ravinder, D. (1992) *J. Mater. Sci. Lett.* **11**, 1498.
[3] Kuanr, K., Singh, P. K., Kishan, P., Kumar, N., Rao, S. L. N., Singh, P. K. and Srivastava, G. P. (1988) *J. Appl. Phys.* **63**(8), 3780.
[4] Cho, S. B., Kang, D. H. and Oh, J. H. (1996) *J. Mater. Sci.* **31**, 4719.
[5] Cheng, K. B., Ramakrishna, S. and Lee, K. C. (2000) *Composites : Part A* **31,** 1039.
[6] Das, N. C., Khastgir, D., Chaki, T. K. and Chakraborty, A. (2000) *Composites : Part A* **31**, 1069.
[7] Kishan, P. Sagar, D. R. and Swarup, P. (1985). *J. Less-Common Met.* **108**, 345.
[8] Mitra, R. Puri, R. K. and Mendiratta, R. G. (1992) *J. Mater. Sci.* **27**, 1275.

[9] Darowicki, K. (1995) *Electrochemica Acta* **40**(4), 439.
[10] Braun, P. B. (1952) *Nature* **170**, 1123.
[11] Went, J. J. and Wijn, P. J. (1951) *Phys. Rev.* **82**, 269.
[12] Kleitz, M. and Kennedy, J. H. (1979) in *Proceedings of the Fast Ion Transport In Solids, Electrodes and Electrolytes*, edited by P. Vashista, J. N. Mundy and G. K. Shenoy (Elsevier, North Holland), p. 185.
[13] Chiang, Y. –M., Lavik, E. B., Kosacki, I. and Tuller, H. L. (1997) *J. Electroceramics*, **1:1**, 7.
[14] West, A. R., Sinclair, D. C. and Hirose, N. (1997) *J. Electroceramics* **1:1**, 65.
[15] J. Fleig and J. Maier, *J. Electroceramics* **1:1**, 73, (1997)
[16] Badwal, S. P. S. (1988) in *Proceeding of the International Seminar on Solid State Ionic Devices*, edited by B. V. R. Chowdari and S. Radhakrishna (World Scientific, Singapore), p. 165.
[17] Anderson, J. C. (1964) *Dielectrics* (Chapman and Hall Ltd., London), p. 94.
[18] Anis, M. K. and Jonscher, A. K. (1993) *J. Mater. Sci.* **28**, 3626.
[19] Jonscher, A. K. (1991) *J. Mater. Sci.* **26**,1618.
[20] Jonscher, A. K. (1995) *Universal Relaxation Law* (Chelsea Dielectric Press Ltd., London, p. 152.
[21] Baker, B. C. and West, A. C. (1997) *J. Electrochem. Soc.* **144**(1), 164.
[22] Jonscher, A. K. (1983) *Dielectric Relaxation in Solids* (Chelsea Dielectric Press Ltd., London), p. 87.
[23] Dissado, L. A. and Hill, R. M. (1980) *Phil. Mag.* **B41**, 625.
[24] Dissado, L. A. and Hill, R. M. (1981) *J. Mater. Sci.* **16**, 1410.